Communication

Thermal and Tensile Properties of Bi-Ag Alloys

JENN-MING SONG, HSIN-YI CHUANG, and TIEN-XIANG WEN

This study investigated the microstructure and properties of Bi-Ag alloys, a novel Pb-free solder for high-temperature applications. The results show that Bi-Ag alloys exhibited a nonequilibrium solidification feature and a considerably large undercooling. An increase in the Ag content effectively raised the tensile strength. However, the elongation in a decreasing order was hypereutectic Bi-11Ag, pure Bi, and then eutectic Bi-2.5Ag. The fracture mode was significantly affected by microstructural characteristics and the strain rate.

DOI: 10.1007/s11661-007-9138-1

Bismuth, rhombohedral in structure with both covalent and metallic bonds, is less commonly used as structural material due to its fragility and poor malleability. In the electronics industry, bismuth is usually applied as an alloying element for solder materials, for example, Sn-Bi, Sn-Ag-Bi, Sn-Zn-Bi, Sn-In-Bi, and Sn-Pb-Bi. The addition of Bi can reduce the melting temperature and improve wetting properties.[1,2] It has been reported that Bi containing solders have the problem of embrittlement under a high strain rate.[3,4] That is, the ductility is drastically degraded when the deformation rate exceeds a critical value. In addition, lift off of Bi bearing surface-finished components from the Cu land of a printed wiring board may occur probably due to Bi segregation near the interface.[5,6]

Recently, a new alloy system, Bi-Ag, has been considered as the replacement for high Pb solders for high-temperature applications (*e.g.*, 95Pb-5Sn, with a melting range from 308 °C to 312 °C).[7–10] One of the basic requirements a high-temperature Pb-free solder should satisfy is the melting range. That is, the solidus should be higher than 260 °C; thus, the solder is capable of surviving secondary reflow at 250 °C, and the liquidus needs to be lower than 400 °C, due to the limitation of the glass transition temperature of the polymeric substrate. Bi-Ag eutectic alloy exhibits an acceptable melting point (the eutectic temperature is 262.5 °C at the eutectic composition, Bi-2.5 wt pct Ag), similar hardness to that of Pb-5Sn, and affordable cost. Thus, it has been developed into die attach solders for power devices and light-emitting diodes (LEDs). However, this solder alloy system still has some demerits of inferior thermal and electrical conductivity as well as poor workability. It has been demonstrated that raising the Ag content of Bi-Ag to 11 wt pct promotes an increase in thermal conductivity.[7] Our recent report[11] revealed that the electrical resistivity of the Bi-11 wt pct Ag alloy is 86.5 $\mu\Omega$-cm, which is much lower than that of the Bi-2.5 wt pct Ag eutectic specimen, 116.5 $\mu\Omega$-cm.

In view of the processing parameters, the melting and solidification behavior of solders should be taken into consideration for alloy development. In addition, mechanical properties play an import role in the solder alloy and strongly affect the manufacturability and reliability. Due to a lack of relevant information, this study investigated thermal and tensile behavior of this Bi-based alloy, in particular the effect of Ag content.

The Bi-Ag alloys with an Ag content of 2.5 wt pct (near eutectic composition) and 11 wt pct (hypereutectic composition), designated as Bi-2.5Ag and Bi-11Ag, respectively, were prepared by melting pure bismuth and pure silver in an arc melting furnace in an argon atmosphere. The alloys were then remelted in an electric furnace and poured into a Y-shaped graphite mold. Pure Bi samples were also prepared for comparison.

The thermal behavior of the alloys was investigated using differential scanning calorimetry (DSC) analysis. The specimens with the weight of 10 or 100 mg were heated to above 300 °C and then cooled to the ambient temperature, with a constant rate of 1 °C/min, 10 °C/min, or 15 °C/min.

Rectangular specimens (gage length section: 20 mm × 5 mm × 2 mm) were prepared to perform tensile tests of bulk solders. The crosshead speed was varied from 0.01 to 0.1 mm/min. The corresponding initial strain rate was from 8.33×10^{-6} to 8.33×10^{-5}.

Figure 1 shows the microstructure of the gravity-cast Bi-Ag alloys. In the eutectic Bi-2.5Ag sample, eutectic cells comprising extremely fine Ag-rich nodules can be observed (Figure 1(a)). Some Ag particles with a slightly larger size are located in the vicinity of eutectic cell boundaries. Remarkably, a nonequilibrium solidification structural feature can be identified. The Bi grains and a few primary Ag particles were found (Figure 1(b)). Figure 1(c) illustrates that, in the Bi-11Ag sample, the populations of irregular primary Ag and Bi grains were increased, while the area fraction of eutectic structure was dramatically reduced.

Figure 2 illustrates the representative DSC results of the 10-mg samples measured at 10 °C/min heating/cooling rate (Figure 2(a)), as well as those of 100-mg samples at 15 °C heating/cooling rate (Figure 2(b)). The testing conditions did not affect the tendency of the DSC curves, but caused a shift in specific temperatures. Upon heating, the temperatures of the endothermal peaks for the eutectic reaction of the two Bi-Ag samples did not differ too much and that for fusion of pure Bi was slightly higher than the others. Due to undercooling, the exothermic peaks upon cooling for all the samples appeared at a lower temperature compared to their

JENN-MING SONG, Assistant Professor, HSIN-YI CHUANG, Graduate Student, and TIEN-XIANG WEN, former Undergraduate Student, are with the Department of Materials Science and Engineering, National Dong Hwa University, Hualien 974, R.O.C. Taiwan. Contact e-mail: samsong@mail.ndhu.edu.tw

Manuscript submitted October 16, 2006.
Article published online June 5, 2007.

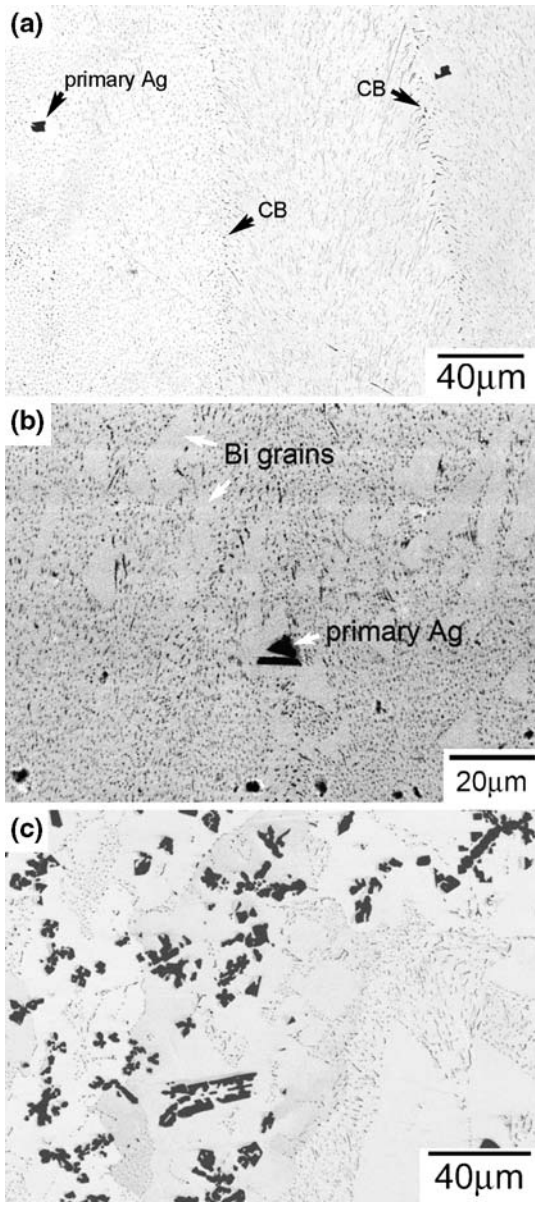

Fig. 1—Microstructure of Bi-Ag alloys: (*a*) and (*b*) Bi-2.5Ag (CB: cell boundary) and (*c*) Bi-11Ag.

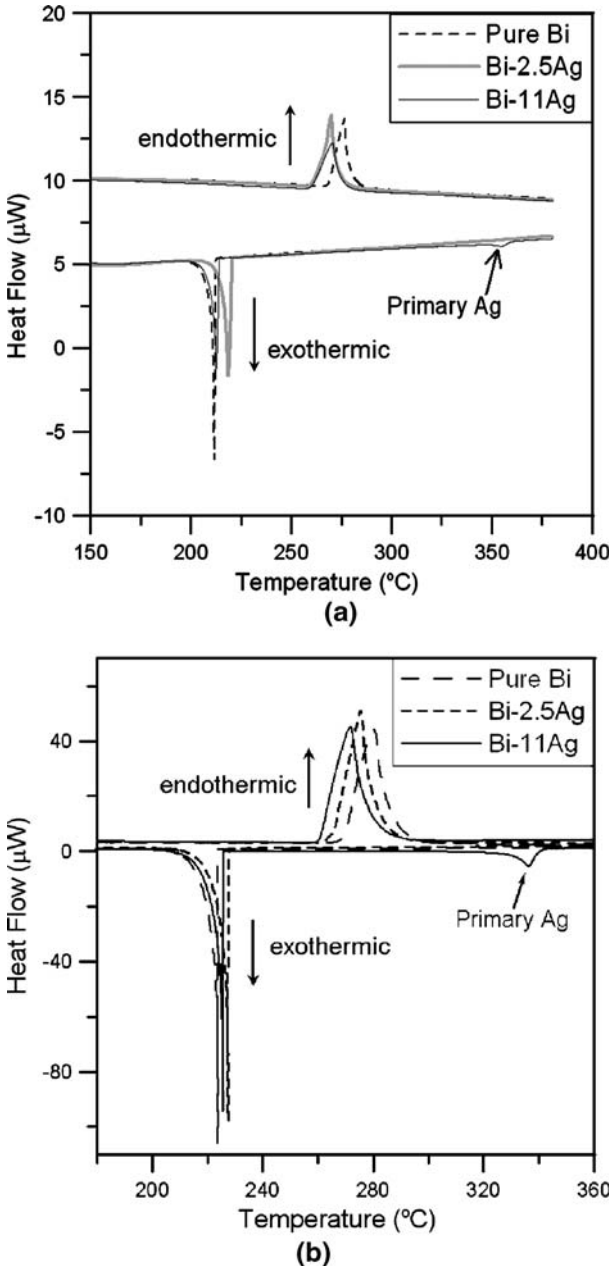

Fig. 2—Representative DSC analysis results under different testing conditions: (*a*) 10-mg samples with a heating/cooling rate of 10 °C/min and (*b*) 100-mg samples with a heating/ cooling rate of 15 °C/min.

endothermal peak, but the reductions in temperature were not identical. The exothermic peak for the eutectic reaction of the Bi-2.5Ag sample was observed at a higher temperature than that for the Bi-11Ag, which was in turn slightly higher than the peak for solidification of pure Bi. During cooling, a small exothermic peak was detected in the DSC curve of the Bi-11Ag at around 350 °C in Figure 2(a) and 340 °C in Figure 2(b). This exothermal behavior was due to the crystallization of the primary Ag phase in the melt.

The transition points and undercooling for each specimen under different testing conditions are listed in Table I. In this study, the degree of undercooling is obtained from the difference in peak temperature between endothermic and exothermal reactions. It is worth noting that, under all the conditions, the undercooling of pure Bi was greater than the Bi-Ag alloys, for which the degree of undercooling might not be related to the Ag content. Table I also reveals that a reduction in the sample weight (sample size) and an increase in the rate of heating/cooling affected the specific temperatures, especially for raising the liquidus temperature upon heating and lowering the peak temperature upon cooling. However, the lowest undercooling measured in this study, 31.9 °C for the Bi-11Ag sample, is still tremendous. This can be ascribed to the rhombohedral structure of Bi, because a large supercooling can be obtained for metals having a more complex crystal structure including Sn, Bi, Ga, and the like.[12]

Table I Specific Temperatures (°C) of the DSC Results underDifferent Testing Conditions*

	T_S-endo	T_P-endo	T_L-endo	T_P-exo	$8T$
Conditions\sample	Pure Bi				
(10 mg-10 °C/min)	264.0	276.5	292.1	211.7	64.8
(100 mg-1 °C/min)	268.0	271.2	273.6	231.2	40.0
(100 mg-15 °C/min)	269.2	280.2	307.4	223.7	56.5
	Bi-2.5Ag				
(10 mg-10 °C/min)	258.2	269.8	285.7	218.4	51.4
(100 mg-1 °C/min)	259.7	263.3	265.8	230.7	32.6
(100 mg-15 °C/min)	265.1	275.5	300.9	227	48.5
	Bi-11Ag				
(10 mg-10 °C/min)	256.5	270.4	285.6	212.4	58.0
(100 mg-1 °C/min)	259.7	263.8	266.2	231.9	31.9
(100 mg-15 °C/min)	260.5	271.7	302.7	225.6	46.1

*(-Endo represents the data from endothermic peaks, and -exo means exothermic peaks. T_P-endo and T_P-exo are ultimate temperature values of the endothermic peaks upon heating and exothermic peaks upon cooling. Their difference represents the degree of undercooling ($8T$). T_S-endo and T_L-endo are, respectively, solidus and liquidus temperatures of the endothermic peaks.

As illustrated in Figure 2, primary Ag started to crystallize at temperatures much higher than the eutectic temperature. The depletion of Ag in the residual liquid resulted from the increased number of primary Ag particles, leading to a limited amount of the eutectic structure and an increased area of Bi grains. The microstructural feature of hypereutectic Bi-Ag is similar to that of hypereutectic Al-Si. That is, primary Si particles, a shell of Al formed around the primary Si, as well as Al dendrites and the eutectics coexisted in the microstructure especially under high cooling rates.[13] The hypoeutectic matrix was due to the nonequilibrium solidification. Loper has suggested that the Al shell surrounding the primary Si may be caused by a divorced eutectic reaction.[14]

Tensile properties are listed in Figure 3. Figure 3(a) illustrates that the tensile strengths, including yield strength and ultimate strength, became greater with an increased Ag content. Interestingly, Figure 3(b) shows that, under all the strain rate conditions, the elongation of the samples in decreasing order was Bi-11Ag, pure Bi, and then Bi-2.5Ag. The elongation of the Bi-2.5Ag specimens was drastically degraded to be less than 10 pct when the strain rate was raised to 4.2×10^{-5} s^{-1} and above. On the other hand, the elongation of the Bi-11Ag and pure Bi remained higher than 20 pct when the tensile test was performed at the highest deformation rate, 8.3×10^{-5} s^{-1}.

Figure 4 shows the tensile fracture surface revealing some differences in fracture modes. It can be observed that, at high strain rates, the Bi-2.5Ag and pure Bi samples possess a smooth flat cleavage surface (Figures 4(a), (c), and (d)). When tensioned under the strain rate of 8.3×10^{-6} s^{-1}, the fracture morphology of these two specimens became more ductile, as shown in Figures 4(b) and (e), a rough distorted surface comprising small facets. Remarkably, such a ductile fracture manner appeared in the Bi-11Ag samples under all the tensile conditions. There might exist a critical elongation of 30 pct for the transition of fracturing mode from brittle to ductile.

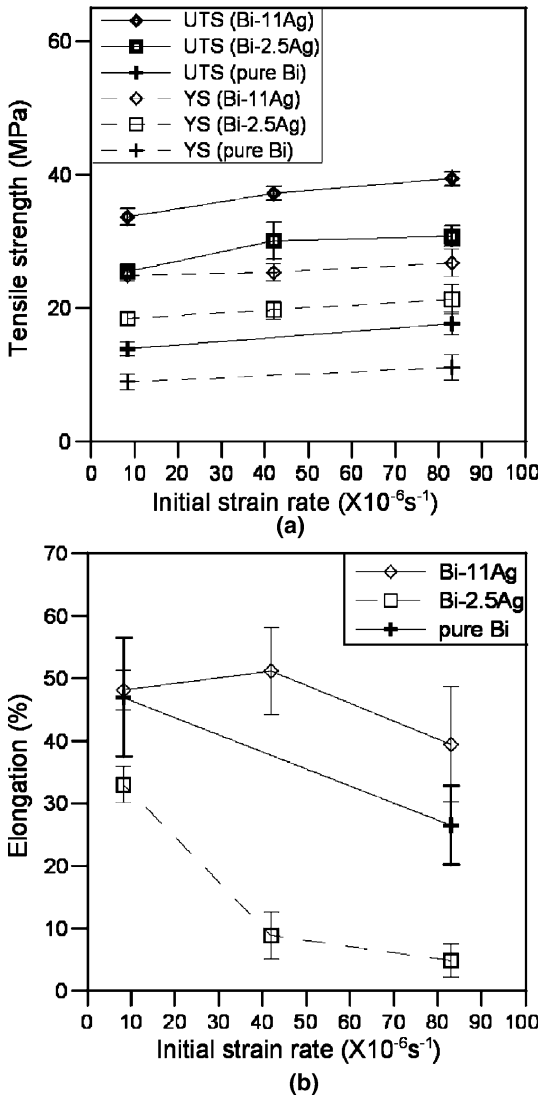

Fig. 3—Tensile properties of bulk Bi-Ag and pure Bi samples: (*a*) tensile strength (YS: yield strength, and UTS: ultimate tensile strength) and (*b*) elongation.

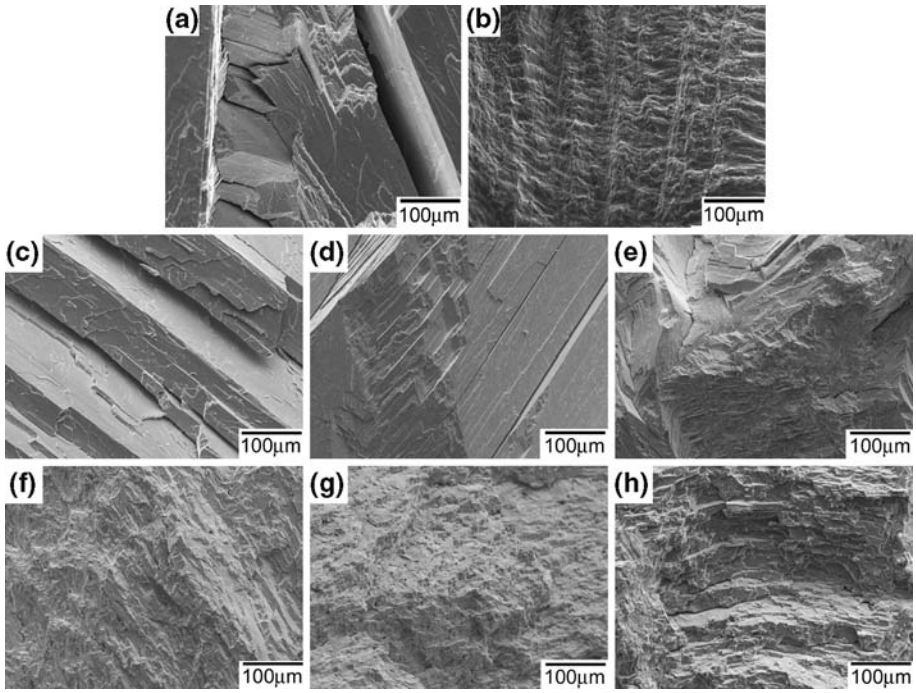

Fig. 4—Tensile fractography of the samples at different strain rates: (*a*) pure Bi, 8.3×10^{-5} s^{-1}; (*b*) pure Bi, 8.3×10^{-6} s^{-1}; (*c*) Bi-2.5Ag, 8×10^{-5} s^{-1}; (*d*) Bi-2.5Ag, 4.2×10^{-5} s^{-1}; (*e*) Bi-2.5Ag, 8.3×10^{-6} s^{-1}; (*f*) Bi-11Ag, 8.3×10^{-5} s^{-1}; (*g*) Bi-11Ag, 4.2×10^{-5} s^{-1}; and (*h*) Bi-11Ag, 8.3×10^{-6} s^{-1}.

Figures 5 and 6 display the deformation structure and crack growth morphology of the tensile fractured samples. Deformation of bismuth by twinning is relatively easy compared to other materials (Schmid factor is 0.48) especially at high deformation rates.[15] However, in this work, no twins were revealed in the deformed areas (Figure 6). Accordingly, the possible deformation mechanism in this case could be considered as dislocation slip on (111) planes rather than twinning.[16] The smooth flat cleavage surfaces shown in Figure 4 were likely (111) plane.[17]

The crack propagation morphology provides further information regarding microstructural effect on tensile behavior. The cross-sectional structure of the fractured Bi-2.5Ag sample (Figure 5(a)) displays long straight cracks propagating zigzag across Bi-Ag eutectic cells when tensioned under the high strain rate condition. On the other hand, primary Ag in the necked region of the Bi-11Ag tended to elongate along the tensile direction and the fracture surface was much more ragged (Figure 5(b)). Magnified structure in Figure 6(a) illustrates that cracks grew directly across the eutectic and proeutectic regions of the Bi-11Ag sample with very few meanders. This indicates that those structures were not able to resist the crack growth effectively. In contrast, the cracks became more tortuous and branching when massive primary Ag was encountered (Figures 6(b) and (c)). It could also be observed that the cracks grew around the primary Ag particles without penetrating them. The preceding observation implies that, besides stunting crack propagation, ductile phase such as primary Ag may accommodate the stress intensity,

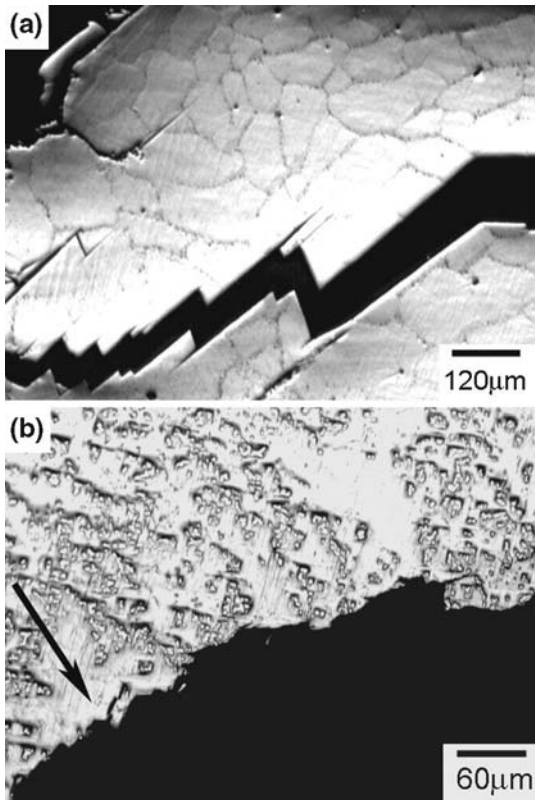

Fig. 5—Microstructure of the necked region of the specimens under a high strain rate of 8.3×10^{-5} s^{-1}: (*a*) Bi-2.5Ag and (*b*) Bi-11Ag (the arrows indicate the tensile direction).

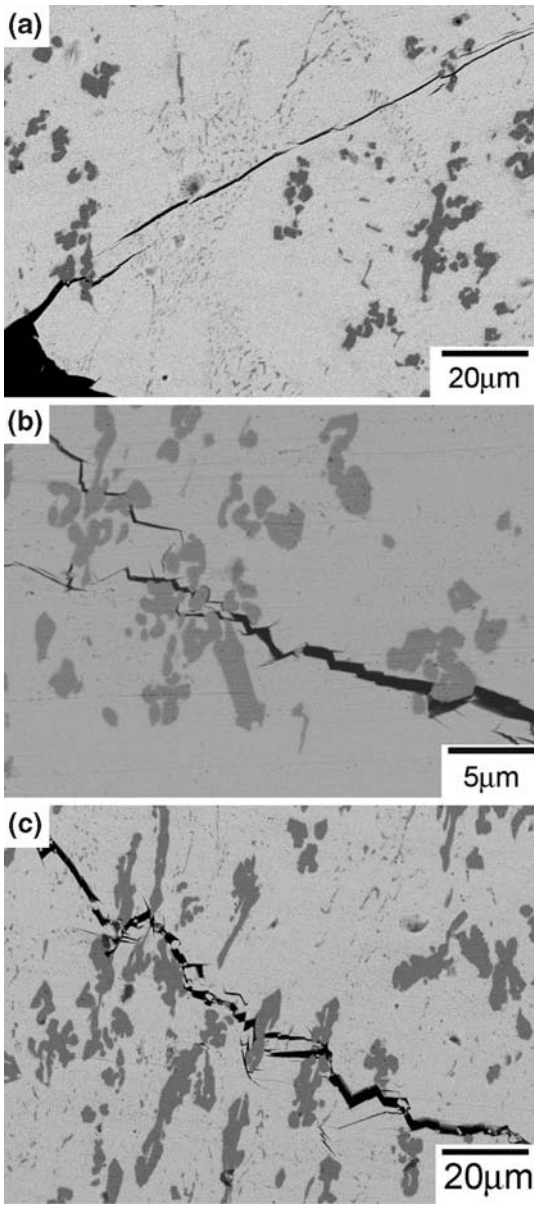

Fig. 6—Crack propagation morphology of the Bi-11Ag sample with different strain rates: (*a*) 8.3×10^{-5} s^{-1}, (*b*) 4.2×10^{-5} s^{-1}, and (*c*) 8.3×10^{-6} s^{-1}.

retard strain localization, and thus improve ductility.[18] However, extremely fine Ag particles within eutectic structure seemed to have no such merit. Because the pure Bi sample possessed a superior ductility than the Bi-2.5Ag, it can be deduced that the eutectic structure had a negative effect on the crack propagation resistance, probably due to crack linking by fine eutectic Ag nodules.

In conclusion, with proper Ag addition, the ductility of brittle Bi could be drastically improved and thus bring about the likelihood of structural materials for microelectronic jointing applications. The Bi-Ag alloys showed a nonequilibrium solidification structural feature. Primary Ag, Bi grains, and Bi-Ag eutectics coexisted in the microstructure. A large undercooling could be obtained upon solidification, and the degree of undercooling of pure Bi was greater than the Bi-Ag alloys. The Ag additions were effective in strengthening for Bi alloys. The Bi-11Ag sample had a greater elongation than that of the pure Bi, which in turn was greater than the Bi-2.5Ag sample under all the strain rate conditions in this study. The massive primary Ag, which has the ability to retard strain localization and stunt crack growth, is probably responsible for the superior ductility of the Bi-11Ag sample at high deformation rates.

This work has been supported by the Chinese National Science Council (Contract No. NSC 95-2221-E-259-014), for which the authors are grateful.

REFERENCES

1. P.T. Vianco and J.A. Rejent: *J. Electron. Mater.*, 1999, vol. 28, p. 1127.
2. P.T. Vianco and J.A. Rejent: *J. Electron. Mater.*, 1999, vol. 28, p. 1138.
3. S. Sengupta, H. Soda, and A. McLean: *J. Mater. Sci.*, 2002, vol. 37, p. 1747.
4. M. McCormack, H.S. Chen, G.W. Kammlott, and S. Jin: *J. Electron. Mater.*, 1997, vol. 26, p. 954.
5. K. Suganuma: *Scripta Mater.*, 1998, vol. 38, p. 1333.
6. H. Takao and H. Hasegawa: *J. Electron. Mater.*, 2001, vol. 30, p. 1060.
7. L.N. Lalena, N.F. Dean, and M.W. Weiser: *J. Electron. Mater.*, 2002, vol. 31, p. 1244.
8. J.H. Kim, S.W. Jeong, and H.M. Lee: *Mater. Trans.*, 2002, vol. 43, p. 1873.
9. M. Rettenmayr, P. Lambracht, B. Kempf, and M. Graff: *Adv. Eng. Mater.*, 2005, vol. 7, p. 965.
10. J.M. Song, H.Y. Chuang, and Z.M. Wu: *J. Electron. Mater.*, 2006, vol. 35, p. 1041.
11. J.M. Song, H.Y. Chuang, Z.M. Wu, and G.W. Lee: *J. Taiwan Vac. Soc.*, 2006, vol. 18, p. 8.
12. *Fundamentals of Physical Metallurgy*, John Wiley and Sons, Inc., New York, NY, 1975, p. 233.
13. H.S. Kang, W.Y. Yoon, K.H. Kim, M.H. Kim, and Y.P. Yoon: *Mater. Sci. Eng. A*, 2005, vol. 404, p. 117.
14. J.C. Weiss and C.R. Loper Jr.: *AFS Trans*, 1987, vol. 95, p. 51.
15. O.M. Ostrikov: *Tech. Phys.*, 1999, vol. 44, p. 597.
16. O.M. Ostrikov and S.N. Dub: *Tech. Phys.*, 2001, vol. 46, p. 549.
17. G. Motoyasu, H. Kadowaki, H. Soda, and A. McLean: *J. Mater. Sci.*, 1999, vol. 34, p. 3893.
18. F. Szuecs, C.P. Kim, and W.L. Johnson: *Acta Mater.*, 2001, vol. 49, p. 1507.